Journal of Fluorescence, Vol. 6, No. 3, 1996

2-Naphthol-Phosphatidylethanolamine: A Fluorescent Phospholipid Analogue for Excited-State Proton Transfer Studies in Membranes

Paolo Neyroz,[1,3] Lorella Franzoni,[2] Carolina Menna,[1] Alberto Spisni,[2] and Lanfranco Masotti[1]

Received August 30, 1995; accepted April 30, 1996

The fluorescence properties of the phospholipid derivative, *N*-[1-(2-naphthol)]-phosphatidylethanolamine (NAPH-PE), have been studied by steady-state and time-resolved fluorescence techniques. The new probe is a naphthol adduct of phosphatidylethanolamine. The emission spectrum of the fluorescent phospholipid depends on the pH and on the proton acceptor concentration as expected for a typical two-state excited-state proton transfer reaction. In ethanol solutions at an apparent pH of 6.7 and in the presence of acetate anion (0.14 *M*), a biexponential decay is obtained from global analysis of the data. The lifetimes, $\tau_1 = 3.9$ ns and $\tau_2 = 6.2$ ns, are constant across the spectral region 350–460 nm. The decay-associated spectra and the species-associated spectra reproduce well the profiles reported for a two-state excited-state proton transfer reaction. The fluorescent phospholipid has been incorporated into dimyristoyllecithin and dipalmitoyllecithin vesicles. Although lower proton transfer is found, the reaction appears to be dependent on the gel-to-liquid-crystalline phase transition of the lipid membrane. In addition, the steady-state anisotropy of NAPH-PE measured as a function of temperature trace the phase transition of the two vesicle systems. Thus, it is shown that the physical state of the bilayer affects a reaction which takes place at the membrane surface. In the presence of acetate ions (0.3 *M*), global analysis, performed in terms of fluorescence decay parameters, recovers preexponential coefficients that are consistent with an excited-state proton transfer reaction. The short lifetime drops from 3.9 to 0.44 ns without significant changes of the longer-lifetime component.

KEY WORDS: 2-Naphthol-phosphatidylethanolamine; excited-state proton transfer; membrane; phospholipid analogue.

INTRODUCTION

The use of fluorescent phospholipid analogues has been extensively used to study the functional and structural properties of biological membranes.[1–6] In general, different kinds of questions can be addressed. For example, based on the chemical structure of phospholipids, a fluorophore can be attached to the acyl chains moiety or to the polar head group,[3] and different regions of the bilayer can be probed (i.e., the acyl core or the lipid–water interface). In addition, all the static and dynamic information contained in a variety of fluorescence experiments (energy transfer, excimer formation, fluorescence anisotropy, and intensity decay measurements) can be used to monitor processes of biological significance

[1] Dipartimento di Biochimica "G. Moruzzi," Sezione di Biochimica Farmaceutica, Universitá degli Studi di Bologna, Bologna, Italy.
[2] Istituto di Chimica Biologica, Facoltá di Medicina e Chirurgia, Universitá degli Studi di Parma, Parma, Italy.
[3] To whom correspondence should be addressed at Dipartimento di Biochimica "G. Moruzzi," Sezione di Biochimica Farmaceutica, Via San Donato, 19/2°, 40126 Bologna, Italy.

1053-0509/96/0900-0127$09.50/0

such as cell fusion,[7,8] lipid lateral diffusion and organization,[9–11] phase separation, and interactions of cations with membrane components.[6,12]

Aromatic alcohols exhibit excited-state ionization constants that differ by several orders of magnitude from those observed in the ground state[13,14] and, hence, will transfer a proton, in the excited state, if suitable conditions (pH, presence of proton acceptor species, etc.) are fulfilled. The kinetics of the excited-state proton transfer reaction of 2-naphthol in aqueous solutions has been studied in great detail and the rate constants of the process have been measured by both static and dynamic fluorescence techniques.[13,15,16] More recently new analytical and experimental approaches have been developed providing resolution of the spectral and kinetics information contained in a time-resolved fluorescence experiment. In particular, procedures have been described to obtain the spectra associated with the recovered decay constants (DAS),[4,17] and the spectra relative to the protonated and deprotonated emitting species (SAS).[11,18]

The use of excited-state proton transfer dyes as biological probes has been described in several preceding reports. Although proteins have been used as a substrate for proton transfer dye conjugation,[19–23] studies on membranes have been carried out only with free dyes.[11,24,25] In addition, with the advancement of new optical technologies in cell biology (i.e., UV lasers, dual-excitation geometries, and dual-emission channel detection systems in cytofluorometry and confocal microscopy), new fluorescent probes with increasing chemical and biological sensitivity may find useful applications.

In this study we present the steady-state and time-resolved fluorescence characterization of a naphthol adduct of phosphatidylethanolamine (PE). The results obtained with the phospholipid derivative in solution show that the new probe undergoes a two-state excited-state proton transfer reaction. Upon incorporation into L-α-(dimyristoyl)lecithin (DML) and L-α-(dipalmitoyl) lecithin (DPL) vesicles, the proton transfer reaction appears to be dependent on the lipid phase transition. Fluorescence intensity and anisotropy results are discussed in terms of dynamics of the lipid bilayer, and more important, they provide clues for understanding signal transduction mechanisms at the membrane surface.

[4] *Abbreviations used*: DAS, decay-associated spectra; DML, L-α-(dimyristoyl) lecithin; DMPE, dimyristoyl-L-α-phosphatidylethanolamine; DOPE, L-α-dioleylphosphatidylethanolamine; DPL, L-α-(dipalmitoyl)lecithin; Et_3N, triethylamine; G-C, gas chromatography; NAPA, 2-hydroxy-1-naphthaldehyde; NAPH-PE, *N*-[1-(2-naphthol)] phosphatidylethanolamine; PE, phosphatidylethanolamine; SAS, species-associated spectra; SUV, small unilamellar vesicles; TLC, thin-layer chromatography.

MATERIALS AND METHODS

The synthesis of the phospholipid derivative, N-[1-(2-naphthol)]phosphatidylethanolamine (NAPH-PE), was carried out as described previously.[26] 2-Hydroxy-1-naphthaldehyde (NAPA) was obtained from Fluka; DML, DPL, L-α-dimyristoylphosphatidylethanolamine (DMPE), and L-α-dioleylphosphatidylethanolamine (DOPE) were from Avanti Polar-Lipids, Inc. The purity of the compounds was verified by thin-layer chromatography (TLC) on heat-activated silica gel 60 plates. Sodium borohydride ($NaBH_4$) and sodium acetate (anhydrous powder) were supplied by Merck and stored at room temperature in a desiccator flask. Triethylamine (Et_3N) from Merck was stored in the dark at 4°C. Triton X-100 was purchased from Sigma Chemical Co. Ethanol, methanol, and chloroform UVasol and GC-HPLC grade (99–99.9% pure) were from Merck. TLC silica gel 60 on aluminum sheets (layer thickness, 0.2 mm) and on glass plates (20 × 20 cm; layer thickness, 0.25 and 0.5 mm) was also purchased from Merck. Sephadex G-50 and Sephadex LH-20 were obtained from Pharmacia Fine Chemicals and used following the instructions of the supplier. The concentration of phospholipid was determined from the phosphorus content.[27] The stoichiometry of NAPH-PE (2-naphthol/PE = 1.05 ± 0.04), was obtained using the molar extinction coefficient of 2-naphthol in ethanol ($\varepsilon_{334} = 2.2 \times 10^3\ M^{-1}\ cm^{-1}$).[26]

The apparent pH of 95% ethanol/water solutions was measured as the pH of water (HPLC-grade, double-distilled water) used to reach the final dilution.

DML and DPL small unilamellar vesicles (SUV) were prepared by sonication in 10 m*M* Tris–HCl, pH 6.7, with 1 m*M* EDTA at 30 and 42°C, respectively, under argon to minimize lipid peroxidation.[28,29] Vesicles were sized by passing the lipid dispersion trough a 1.5 × 25-cm Sephadex G-50 (fine-grade) gel filtration column at 4°C[30] and equilibrated with the same solution of the vesicle suspension. Labeled vesicles were prepared by mixing the unlabeled phospholipid, DML or DPL, with NAPH-PE (molar ratio, 60:1 to 200:1) prior to the vesicle formation by sonication. Occasionally, an alternative procedure was used by adding small aliquots (5–10 μl) of NAPH-PE dissolved in ethanol to unlabeled liposomes previously formed by sonication. When required these vesicles were finally loaded on Sephadex G-50, at 4°C, to separate the labeled vesicles from the

free NAPH-PE. Experiments in the presence of acetate ions were carried out by passing the sonicated vesicles through a gel-filtration column equilibrated with a buffer (10 m*M* Tris–HCl, pH 6.7, 1 m*M* EDTA) containing 0.3 *M* sodium acetate and resuspending aliquots of the pooled vesicles in the same buffer.

For the samples containing increasing acetate concentrations, a 4 *M* stock solution was prepared and the pH adjusted to 6.7 by adding HCl; this stock solution was used to prepare the samples at the desired acetate concentration. Before fluorescence measurements were made the pH of all the samples was checked and adjusted to the experimental pH, if required. In the case of long-lasting time-resolved fluorescence measurements, care was taken to check the pH at the end of each experiment. All fluorescence studies were carried out at 15°C unless stated otherwise.

Fluorescence Spectroscopy Measurements. Technical steady-state fluorescence excitation and emission spectra were obtained with a Perkin–Elmer MPF-44A spectrophotometer. For the fluorescence measurements of pure NAPH-PE in organic solvents, solutions were prepared by adding 8 μl of an ethanol solution of the product to 2 ml of ethanol (final concentration $\approx 1 \times 10^{-5}$ *M*). Samples were excited at 337 nm. The excitation and emission bandwidths were set at 4 nm. The absorbance for all the fluorescence samples at 337 nm was kept less than 0.1 to avoid inner filter effects.[31] The steady-state emission anisotropy was determined as described previously[32,33] using two linear polarizers, Polaroid HNP'B (Polaroid Corp., Cambridge, MA) placed in the excitation and emission paths. The polarized components of the fluorescence intensities were recorded in the "ratio mode" using excitation and emission wavelengths of 337 and 370 nm, respectively.

Nanosecond time-resolved fluorescence measurements were carried out by the time-correlated single-photon counting method.[33–35] A home-built instrument, with a thyratron-gated nitrogen flash lamp (Model F199, Edinburgh Instruments, U.K.) as exciting source and with the typical Ortec fast electronic modules (EG&G Ortec, TN, U.S.A.), was used to collect the fluorescence decay curves. The emission decay of anthracene in methanol was measured in a separate experiment and used as monoexponential standard to correct for the wavelength-dependent transit time of the photomultiplier.[36] Typically, samples were excited at 337 nm and 10^4 counts was collected in the peak's channel. The excitation and emission band widths were set at 4 nm, with the exception of the decay curves collected to extract the DAS and the SAS, where excitation and emission band widths of 8 and 32 nm, respectively, were used.

Data Analysis. Decay data were analyzed by the method of nonlinear least squares[37,38] implemented to produce the simultaneous analysis of multiple decay curves, *global analysis.*[39] A multiexponential function of the form

$$I(t) = \sum_{n=1}^{i} \alpha_i \cdot e^{-t/\tau_i} \qquad (1)$$

was used to describe the time dependence of the fluorescence intensity, $I(t)$, to recover the preexponential coefficients, α_i, and the fluorescence lifetime, τ_i. In this approximation, the parameter $\alpha_i(\lambda)$ represents the intensity amplitude observed at the emission wavelength, λ, and associated with the decay constant, τ_i. The best fit between the theoretical curve and the data was evaluated from the plot of the residuals, the autocorrelation function of the residuals, and the reduced chi-square.[37]

The DAS were obtained by the global DAS procedure as described previously,[40] and the linkage of the decay constants across the entire spectral region was used to derive the preexponential terms that represent each DAS. The data obtained in the presence of liposomes were corrected for the scattering contribution by adding a very short component (0.01 ns) to the fluorescence decay model. The SAS were obtained following the procedure described by Davenport *et al.*[11]

RESULTS

Fluorescence Measurements in Solution

Steady-State Fluorescence. Figure 1 shows a kinetic scheme for a reversible two-state excited-state reaction. With k_{01} and k_{02} are the rate constants for all the deactivation processes to go from ROH* and RO^-* to ROH and RO^-, respectively. k_{21} and k_{12} represent the rate constants for the ground-state ionization system, while k_{21}^* and k_{12}^* represent the rate constants for the excited-state reactions. A similar scheme was proposed to explain the excited-state proton transfer reaction of 2-naphthol.[13,16] To consider this specific case, in the general representation of Fig. 1, ROH and ROH* indicate the protonated NAPH-PE species in the ground state and in the excited state, respectively, while RO^- and RO^-* represent the relative deprotonated species. Based on the Föster cycle,[13,40] values of 9.49 and 2.89 have been determined for the pK_a and the pK_a^* of 2-naphthol,[42] while values of 8.42 and 1.81 have been calculated for the pK_a and the pK_a^* of the model compound *N*-[1-(2-naphthol)] phosphoethanolamine, respectively.[26] In Fig. 2 the ex-

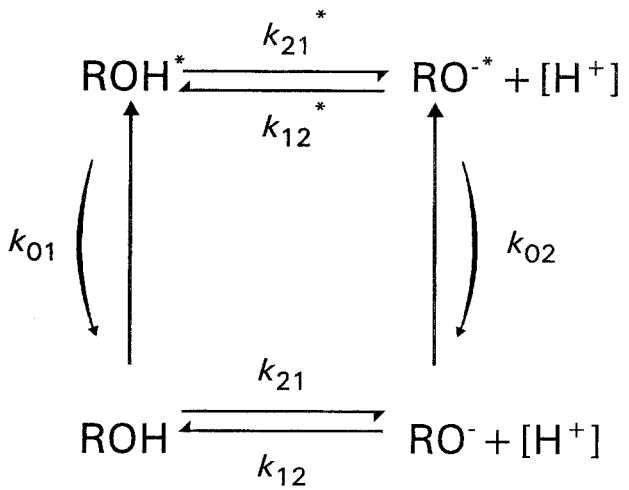

Fig. 1. Kinetic scheme for two-state excited-state reactions. ROH and ROH* represent the protonated NAPH-PE species in the singlet ground state and in the first excited singlet state, respectively, while RO^- and RO^-* represent the corresponding deprotonated species. The rate constants are explained in the text.

citation (Fig. 2*A*) and the emission (Fig. 2*B*) spectra of protonated and deprotonated NAPH-PE obtained in ethanol solutions in the presence of HCl (pH ~2.0) (*solid line*) and NaOH (pH ~12.0) (*dashed line*), respectively, are reported. In the figure the solid-line emission spectrum essentially represents the fluorescence from the excited ROH species, and the dashed-line emission spectrum the fluorescence from the RO^- species.

In Fig. 3, the fluorescence emission spectra of NAPH-PE, obtained at an apparent pH of 6.7 in ethanol and in the absence and the presence of acetate, are shown. In the presence of increasing concentrations of acetate the contribution of the ionized species to the steady-state fluorescence spectrum becomes apparent as expected for a typical two-state excited-state proton transfer reaction.

Time-Resolved Fluorescence. At the initial boundary conditions (in the scheme of Fig. 1, only ROH is directly excited, $[RO^-*] = 0$ at $t = 0$), the fluorescence decay of species ROH* and RO^-* can be expressed as[16]

$$I_{ROH}(t, \lambda) = \alpha_{11}(\lambda) \cdot e^{-t/\tau_1} + \alpha_{21}(\lambda) \cdot e^{-t/\tau_2} \quad (2)$$

$$I_{RO^-}(t, \lambda) = \alpha_{12}(\lambda) \cdot e^{-t/\tau_1} + \alpha_{22}(\lambda) \cdot e^{-t/\tau_2} \quad (3)$$

The decay constants, τ_1 and τ_2, are identical for emission from both species and the preexponential terms depend on the rate constants describing the excited-state process. In particular, the amplitudes associated with the decay of the RO^-* state are equal in magnitude and opposite in sign ($-\alpha_{12} = \alpha_{22}$).

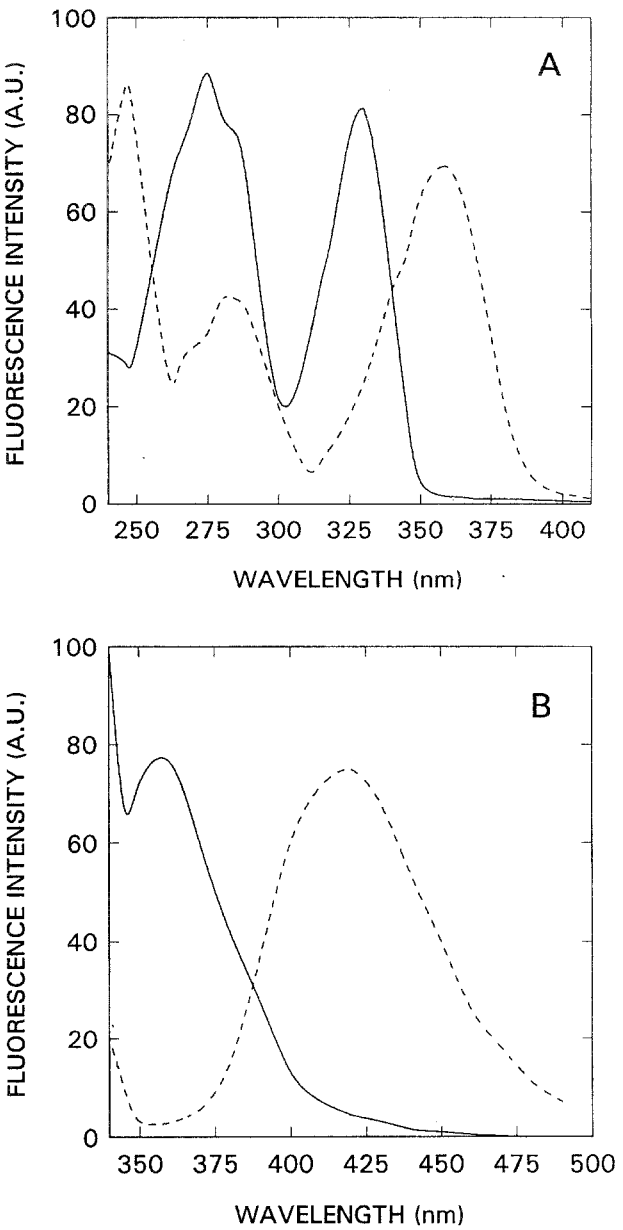

Fig. 2. (A) Normalized excitation fluorescence spectra of NAPH-PE (1×10^{-5} *M*) in 95% ethanol solutions in the presence of hydrochloric acid (*solid line*) and sodium hydroxide (*dashed line*). The emission wavelengths were 360 and 420 nm, respectively. (B) Normalized emission fluorescence spectra of NAPH-PE in 95% ethanol solutions under the same conditions. The excitation wavelengths were 337 and 360 nm, respectively, and the emission band widths were set at 4 nm.

Fluorescence decay measurements of NAPH-PE were carried out in 95% ethanol solution at pH 6.7 and in the presence of 0.14 *M* sodium acetate. The fluorescence decay data obtained at the two emission wavelengths of 360 and 430 nm were first analyzed individually (*single-curve procedure*) with free-floating

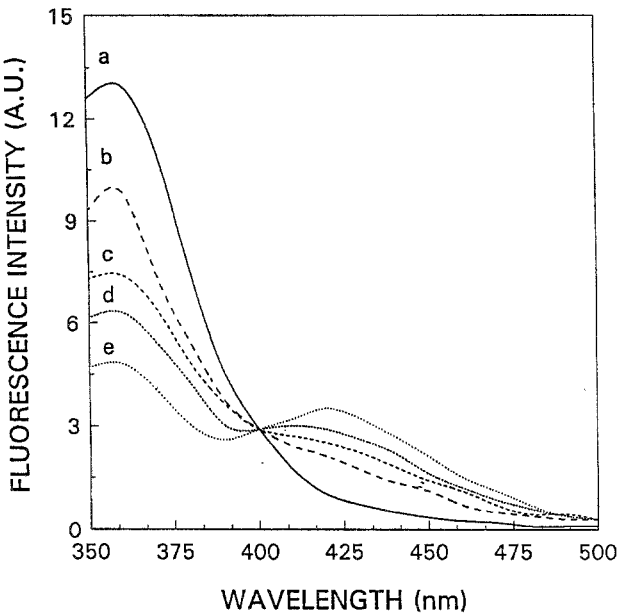

Fig. 3. Emission spectra of NAPH-PE in 95% ethanol solutions at an apparent pH of 6.7, in the presence of (a) no sodium acetate and (b) 0.007 *M*, (c) 0.018 *M*, (d) 0.034 *M*, and (e) 0.085 *M* sodium acetate. The excitation wavelength was 337 nm and the excitation and emission band widths were set at 4 nm.

decay parameters. The results of the time-resolved fluorescence experiments recovered by this kind of analysis are reported in Table I together with the results of the global method used to analyze simultaneously the two decay curves with linked lifetimes. The best fit to the experimental data was found for a biexponential decay at both emission wavelengths studied. At 360 nm, the preexponential terms recovered by single-curve analysis were both positive, with the predominant weight of a single decay time constant of 4.8 ns. At 430 nm the recovered preexponential terms were close in magnitude and opposite in sign, suggesting the existence of excited-state reactions. The small difference found in the amplitudes implies that some of the protonated species also contributed to the emission decay at 430 nm. Global analysis of the NAPH-PE decay curves obtained at 360 and 430 nm revealed two decay times of 3.9 and 6.2 ns, consistent with an essentially irreversible two-state excited-state process.

To test the apparent inconsistencies between the results of the single-curve analysis and the results of the global analysis, the same data were analyzed by the single-curve procedure where one lifetime was fixed to the value recovered by the global method. The results obtained from these trials are also reported in Table I. It is evident that fluorescence decay parameters consistent with an excited-state reaction are recovered by this type of single-curve procedure and that they are associated with a moderate improvement of the statistics of the experiment obtained at 360 nm ($\chi^2 = 1.11$).

The dependence of the preexponential terms on the excited-state reaction rate constants determines the ability to discriminate between different excited-state mechanisms based on the information contained in the resolved DAS (the spectral distribution of the preexponentials associated with each lifetime). Depending on the inequality between the combined rate constants X and Y ($X = k_{01} + k_{21}^*$ and $Y = k_{02} + k_{12}^*$ [H^+]), two DAS features can be obtained, reflecting the two possible cases of two-state excited-state mechanisms, namely, when $X > Y$ and when $Y > X$.[11]

Twelve decay curves were obtained by stepping the emission monochromator every 10 nm in the spectral region 350–460 nm. The experimental curves were analyzed by a global procedure with the two decay constants, τ_1 and τ_2, linked across the decay surface. The DAS derived from the preexponential terms recovered by the global analysis are presented in Fig. 4*A*. Two fluorescence lifetimes of 3.95 and 6.11 ns were obtained, in good agreement with the results reported in Table I. The positive–negative DAS was associated with the short lifetime and contributed in the ROH* spectral region. The positive DAS was associated with the longer lifetime and contributed in the RO^-* spectral region. Such a distribution of the preexponential terms as a function of wavelength, as well as the decay constants found for NAPH-PE, is characteristic of an essentially irreversible two-state excited-state reaction with $X > Y$ ($X = 2.6 \times 10^8$ s^{-1} for $\tau_1 = 3.9$ ns and $Y = 1.6 \times 10^8$ s^{-1} for $\tau_2 = 6.2$ ns), as in the case of 2-naphthol.

Two methods have been described to extract the SAS.[11,18] In the present work we used the method outlined by Davenport *et al.*[11] to obtain the SAS from the DAS. In Fig. 4B, the SAS resolved for ROH* and RO^-* are shown. The blue spectrum represents the emission from ROH* and was obtained by the sum of the two lifetimes' DAS, while the red spectrum represents the emission from RO^-* and was obtained directly by the longer lifetime's DAS.

Fluorescence Measurements in Vesicles

Steady-State Fluorescence. Studies were performed to examine the fluorescence properties of NAPH-PE in DML ($T_c^* \approx 24$°C) and DPL ($T_c \approx 40$°C) SUV. The labeled vesicles were prepared in 10 m*M* Tris–HCl, 1 m*M* EDTA at pH 6.7 (see Materials and Methods) and resuspended both in the absence and in the presence of

Table I. Fluorescence Decay Parameters of NAPH-PE as a Function of Wavelength[a]

Sample	Emission (nm)	α_1	τ_1 (ns)	α_2	τ_2 (ns)	χ^2
NAPH-PE	360[b]	0.09	2.59	0.27	4.81	1.15
	430[b]	−0.09	2.34	0.13	6.84	1.28
NAPH-PE	360[c]	0.30	3.88	0.05	6.20	1.42
	430[c]	−0.17	3.88	0.23	6.20	1.42
NAPH-PE	360[d]	0.26	3.88	0.009	5.75	1.11
	430[d]	−0.16	3.88	0.26	6.36	1.31

[a]Samples ($\approx 0.5\times10^{-5}$ *M*) were prepared in ethanol at pH 6.7, in the presence of 0.14 *M* sodium acetate. The data were analyzed as a sum of exponential and the reported χ^2, the residuals, and the autocorrelation plots were used to judge the goodness of the fit.

[b]Single-curve analysis (χ^2 = "local").

[c]Global analysis (χ^2 = "global reduced"). Decay curves were corrected for spectral distortions [16]. Curves were properly time-shifted prior to the correction; the χ^2 values refer to the analysis of the corrected data. When global analysis was performed on the raw decay data, the recovered "global reduced" χ^2 was 1.21 with $\alpha_1 = -0.16$ and $\alpha_2 = 0.30$. The mean lifetime, $\langle\tau\rangle$, measured at a 430-nm emission wavelength and calculated as $\Sigma|\alpha_i|\cdot;|\tau_i^2|/\Sigma|\alpha_i|\cdot|\tau_i|$, was 5.47 ns.

[d]Results of single-curve analyses with fixed τ_1.

proton acceptors. At the acetate concentrations used in the solution experiments (0.007–0.14 *M*), lower proton transfer was observed in the presence of lipids (see below), and 0.3 *M* sodium acetate was used to investigate the excited-state proton transfer reaction of NAPH-PE at the membrane surfaces. At 360 nm the fluorescence intensity of NAPH-PE incorporated into the vesicles was about 70% higher than the same amount of NAPH-PE suspended in aqueous solution.

The steady-state emission spectra recorded as a function of temperature with both DML (Fig. 5*A*) and DPL (Fig. 5*B*) liposomes, are shown in Fig. 5. The profiles of these spectra show that, once inserted into the bilayer, the extent of the NAPH-PE proton transfer reaction in the presence of proton acceptors is decreased compared with the results obtained with NAPH-PE in ethanol solution, at 15°C (Fig. 3). In addition, in Fig. 5 it is shown how the extent of the deprotonation appears to be temperature dependent. At 9 and 10°C, well below the phase transition of both lipids, the emission spectra are mostly originated by the protonated species. At 25 and 29°C, above the phase transition of DML and below the phase transition of DPL, the emission spectrum of NAPH-PE in DML exhibits a significant contribution of the deprotonated species at 420 nm, while a much smaller increment of the intensity at 420 nm is evident in DPL vesicles. Finally, at 42 and 47°C, above the phase transition of both lipids, the emission spectra of NAPH-PE exhibit the contribution of the deprotonated species in both DML and DPL vesicles.

The effect of the lipid bilayer's phase transition on the proton transfer reaction is shown in Figs. 6A and B, where the ratios of the fluorescence intensities measured at 360 nm *vs* the fluorescence intensities measured at 420 nm and the sole intensity observed at 420 nm are plotted as a function of temperature. It can be seen how the spectral changes due to the presence of the proton acceptor molecules are influenced by the lipid phase transition.

As mentioned above, the experiments described in Figs. 5 and 6 were obtained with vesicles prepared in the absence of acetate, and the proton acceptor molecules were added to the external medium. However, it should be pointed out that in the labeled vesicles the lipid-bound dye is located at both the outside and the inside faces of the liposome. In fact, experiments were also carried out with vesicles prepared in the presence of 0.3 *M* sodium acetate (loaded vesicles). With these vesicles the proton transfer behavior of NAPH-PE was tested both in the presence and in the absence of acetate anions in the external medium. In the first case, no significant differences were observed from the data presented in Figs. 5 and 6, while in the second case very poor proton transfer was observed.

To uncover the possible origins of the limited NAPH-PE proton transfer reaction in the lipid bilayer, Triton X-100 (final concentration, 0.5%) was added to a sample of NAPH-PE-DML suspended in the presence of 0.3 *M* sodium acetate. The result is presented in Fig. 7. It is evident how the disruption of liposomes into mixed

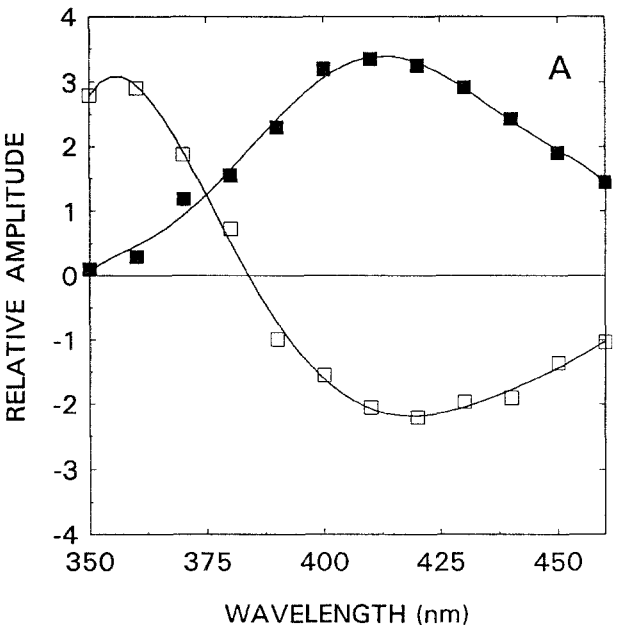

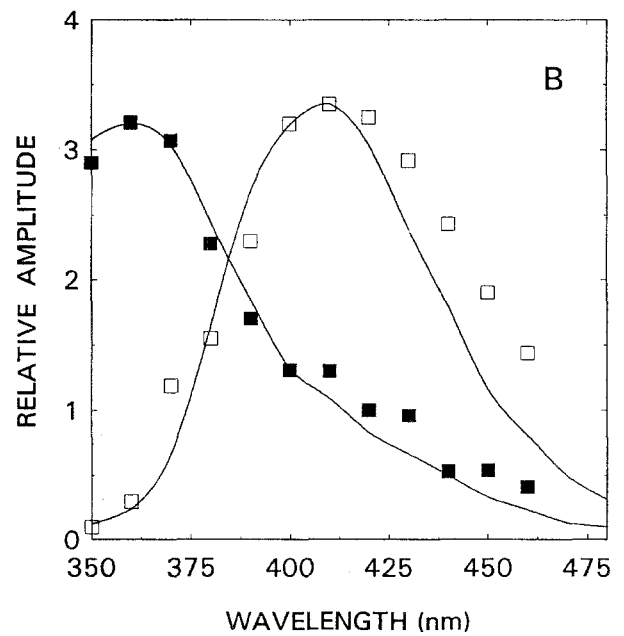

Fig. 4. Time-resolved spectral resolution of NAPH-PE fluorescence emission in 95% ethanol at an apparent pH of 6.7 and in the presence of 0.14 *M* sodium acetate. The excitation wavelength was 337 nm, with excitation and emission band widths set at 8 and 32 nm, respectively. (*A*) Decay-associated fluorescence emission spectra (DAS). The DAS (preexponential) of the short-decay component (□) and the long-decay component (■) were obtained by the global DAS procedure. The solid lines simply represent spline curves through the symbols. The recovered lifetimes were τ_1 = 3.95 ns and τ_2 = 6.11 ns. The global reduced χ^2 was 1.51. (*B*) Species-associated spectra (SAS) obtained from the DAS presented in *A*. The SAS for the ROH^{-*} species (■) is simply the sum of the two-lifetime DAS. The SAS for the RO^{-*} species (■) is obtained directly from the long-lifetime DAS. The solid lines are the technical steady-state spectra obtained from Fig. 3 (line b), for the naphthol species in the presence of acetate and from Fig. 2B for the naphtholate species.

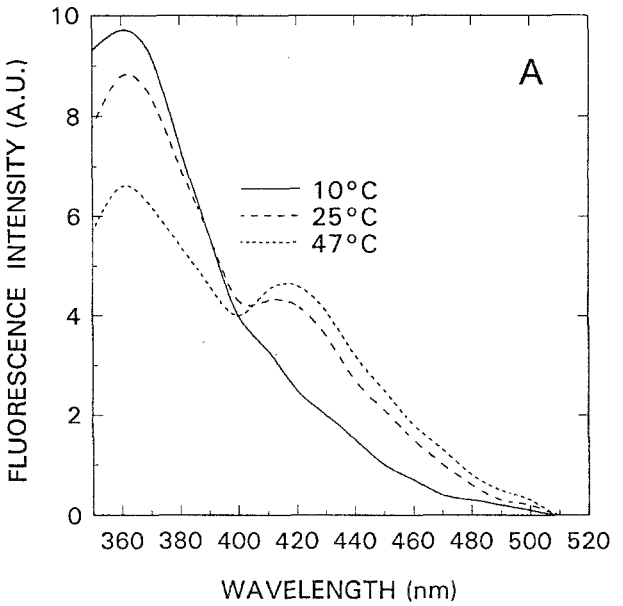

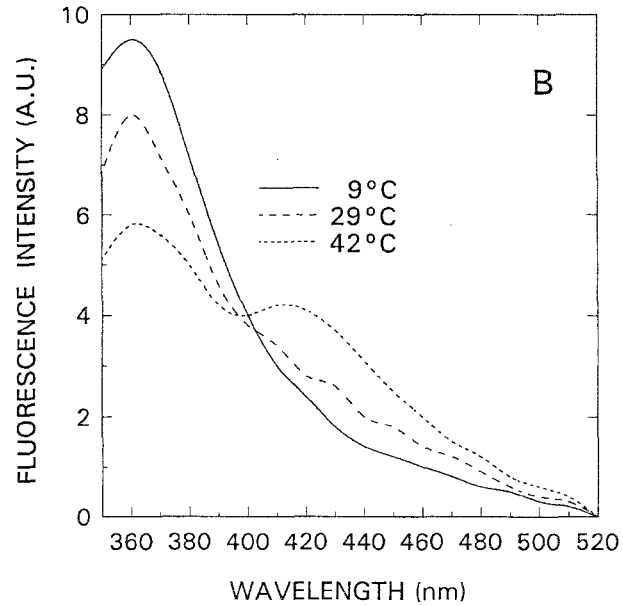

Fig. 5. Steady-state fluorescence emission spectra of NAPH-PE incorporated in DML (*A*) and DPL (*B*) vesicles, as a function of temperature. The vesicles (≈1.5 m*M*; molar labeling ratio, 1:200), prepared in 10 m*M* Tris–HCl, 1 m*M* EDTA, at pH 6.7, were suspended in the same buffer in the presence of 0.3 *M* sodium acetate. The excitation wavelength was 337 nm and the excitation and emission band widths were 4 nm each.

detergent–NAPH-PE micelles results in a significant increase in the accessibility of the probe to the proton acceptor molecules.

To investigate the nature of the NAPH-PE/lipid interaction and to evaluate the sensitivity of NAPH-PE to

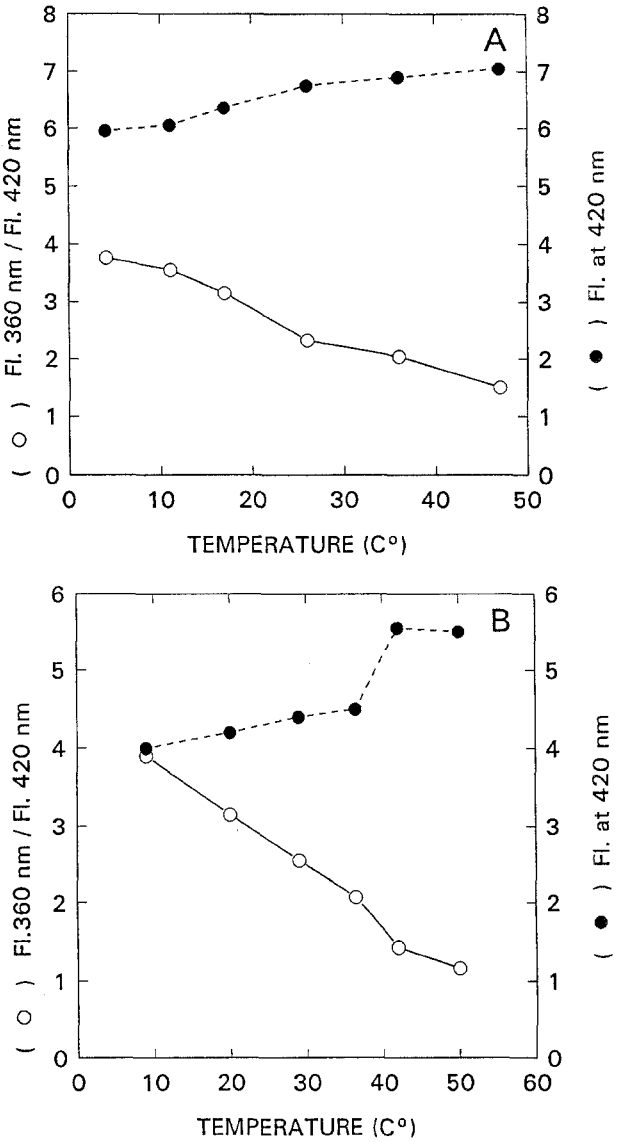

Fig. 6. Changes of the fluorescence intensity of NAPH-PE incorporated in DML (*A*) and DPL (*B*) liposomes, in the presence of 0.3 *M* sodium acetate, as a function of temperature. The *open-symbol* data are expressed as the ratio of the fluorescence intensity measured at 360 and 420 nm. The filled *symbols* are fluorescence intensities measured at 420 nm. The excitation wavelength was 337 nm and the excitation and emission band widths were 4 nm each.

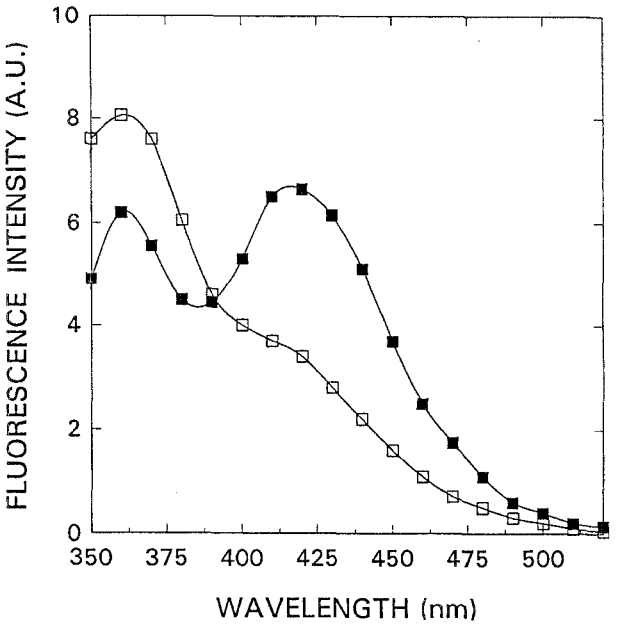

Fig. 7. Steady-state emission spectra of NAPH-PE incorporated in DML vesicles recorded in the absence (□) and in the presence (■) of Triton X-100 (0.5%), at 20°C. All the other conditions were the same as for Fig. 5.

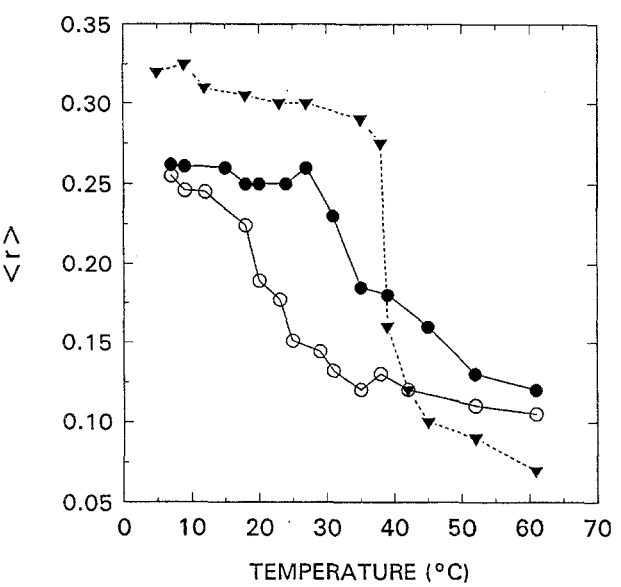

Fig. 8. Steady-state anisotropy, $\langle r \rangle$, of NAPH-PE incorporated into DML (○) and DPL (●) vesicles measured as function of temperature. The excitation wavelength was 337 nm and emission was observed at 370 nm. For comparison, steady-state anisotropy measurements obtained with DPH incorporated in DPL (▼) are also shown.

report the physical state of the bilayer, steady-state anisotropy measurements were performed with the labeled phospholipid incorporated into DML and DPL vesicles. Since the fluorescence anisotropy of a probe undergoing an excited-state reaction may be complex, the emission was observed in the protonated species band, at pH 6.0, and in the absence of acetate anions. In Fig. 8, the results obtained as a function of temperature are shown. In the same figure the data obtained with DPH, incorporated in DPL, are also reported for comparison. By increasing the

Table II. Fluorescence Decay Parameters of NAPH-PE in DML Vesicles as a Function of Wavelength[a]

Sample	Emission (nm)	α_1	τ_1 (ns)	α_2	τ_2 (ns)	χ^2
NAPH-PE	360[b]	0.34	0.44	0.02	5.86	1.58
	430[b]	−0.29	0.44	0.29	5.86	1.58

[a]DML vesicles were resuspended in 10 m*M* Tris–HCl, 1 m*M* EDTA, at pH 6.7, in the presence of 0.3 *M* sodium acetate. The excitation wavelength was 337 nm and the excitation and emission band widths were 4 nm each.
[b]Global analysis (χ^2 = "global reduced"). The mean lifetime, $\langle\tau\rangle$, measured at a 430-nm emission wavelength and calculated as $\Sigma|\alpha_i|\cdot|\tau_i^2|/\Sigma|\alpha_i|\cdot|\tau_i|$, was 5.48 ns.

temperature, NAPH-PE steady-state anisotropy decreases with a profile which follows the phase transitions of DML and DPL. For instance, in the case of DPL, although the phase transition traced by NAPH-PE is broader, it corresponds well to the phase transition revealed by DPH, which has been considered as a typical fluorescent dye used to probe the bilayer phase transition.[42]

Time-Resolved Fluorescence. In spite of the low proton transfer detected in the presence of lipid membranes, the fluorescence decay of NAPH-PE, incorporated in DML liposomes, was measured at two emission wavelengths, 360 and 430 nm, at 28°C, and in the presence of 0.3 *M* sodium acetate. The data collected at 360 nm were corrected for the scattering contribution. The results obtained are presented in Table II. It is shown that the decay observed at 430 nm reproduces well the preexponential term pattern, $-\alpha_{12} = \alpha_{22}$ (see above), which indicates the existence of an excited-state proton transfer reaction. On the other hand, while the long lifetime is only slightly affected (5.9 *vs* 6.2 ns), the short lifetime is strongly quenched (0.4 *vs* 3.9 ns), compared with the data obtained with NAPH-PE dissolved in ethanol. This result corresponds to a 10-fold raise of the combined rate constant X and no significant change of Y($X = 23 \times 10^2\ s^{-1}$ and $Y = 1.7 \times 10^2\ s^{-1}$).

DISCUSSION

The multidimensional character of fluorescence spectroscopy provides an ideal tool to study biological compartments if fluorophores are bound to specific macromolecular loci. In this paper the fluorescence properties of the 2-naphthol phospholipid adduct have been studied by steady-state and time-resolved techniques.

Steady-state fluorescence measurements of NAPH-PE in ethanol and in the presence of increasing concentrations of acetate ions as proton acceptors (Fig. 3) have demonstrated a typical excited-state proton transfer behavior.

Together with the information contained in the steady-state fluorescence experiments, more details on the system under investigation can be extracted by time-resolved techniques. In this regard, analytical expressions have been derived, which relate the parameters of the fluorescence decay processes to the rate constants describing the excited-state reactions,[16,44] and nanosecond time-resolved measurements have been used extensively to study the kinetics of these reactions.[16,19] In the present work the fluorescence decay of the 2-naphthol-conjugated phospholipid has been measured in 95% ethanol in the presence of acetate ions. Fluorescence decay parameters, consistent with a two-state excited-state proton transfer reaction, have been recovered by global analysis. In particular, in the spectral region where the contribution of the deprotonated species is predominant (see Table I), a negative preexponential term was required to obtain the best fit to the experimental data, indicating the existance of an underlying excited-state reacton. Simultaneous analysis of multiple fluorescence decay experiments has been exploited to increase the ability to recover the parameters of complex emission processes as well as the spectra associated with each component of a mixture (i.e., ground-state heterogeneity).[39,45] However, in the case of excited-state reactions, the DAS do not represent the actual spectra of the individual species in solution.[18] In spite of this fact, Davenport *et al.*[11] have indicated that, under unperturbed experimental conditions and in the absence of special assumptions, DAS and their lifetimes represent a significant information, and SAS can be readily derived from DAS. From these data, kinetic information can be extracted, which enable to discrimination between different kinetic systems.

The lifetime-associated spectra of NAPH-PE (Fig. 4*A*) and the recovered decay constants are diagnostic of a two-state excited-state proton transfer process, in which deactivation from ROH* proceeds faster than deactivation from RO^-* (the combined rate constant X is about twice Y; see Results).

In addition, the SAS recovered for the ROH* and RO^{-}* species (Fig. 4*B*) reproduce well the spectra obtained by the steady-state technique. Thus, our experiments show that the excited-state reaction of NAPH-PE follows the same kinetic behavior as the parent molecule 2-naphthol.[16]

Excited-state proton transfer fluorescent probes have been used increasingly to study the molecular microenvironments of biological systems.[11,16,19,21–24] Following the synthesis of NAPH-PE and its chemical characterization,[26] we have now investigated the photophysical properties of NAPH-PE inserted into lipid vesicles.

Upon incorporation into liposomes, the relative quantum yield of NAPH-PE is not changed with respect to the relative quantum yield measured in ethanol ($\langle\tau\rangle$ = 5.48 ns vs $\langle\tau\rangle$ = 5.47 ns; see Tables I and II). On the other hand, the fluorescence intensity of NAPH-PE observed with labeled vesicles is significantly higher than the fluorescence intensity observed with free NAPH-PE simply suspended in aqueous solution.

When sodium acetate is added to the liposome suspension (Fig. 5), the extent of the excited-state proton transfer is decreased with respect to that obtained in ethanol solution (Fig. 3). This is a common observation. Similar results have been reported by Davenport *et al.*[11] for equilenin and dihydroequilenin and by Selinger and Harris[46] for 2-naphthol intercalated in anionic micelles. In the first case, the results have been explained by the effect of the lipid bilayer in shielding the excited molecules from the acetate anion, whereas in the second case, the result has been explained by diminished proton acceptor activity of the acetate anion in the presence of the hydrophobic lipid membrane. The evident increase in emission at 420 nm upon disruption of the lipid bilayer by addition of the nonionic surfactant Triton X-100 (Fig. 7), in the presence of proton acceptors, demonstrates that NAPH-PE can be readily ionized when dispersed in nonionic micelles. Thus, this evidence is in agreement with the interpretation provided by Davenport *et al.*[11] for small molecules incorporated in lipid bilayers and seems to exclude other mechanisms such as a solvent effect (i.e., water *vs* ethanol). In addition, evidence for the existence of a kinetic barrier for proton transfer at the membrane interfaces of planar bilayer lipid membranes has been provided by Antonenko *et al.*[47]

It has been pointed out under Results that the data presented in Figs. 5 and 6 were obtained with vesicles to which proton acceptor molecules were added to the external solvent. Under these conditions, the diminished proton transfer could be apparent, namely, arising from a relative major contribution of protonated species located at the internal leaflet of the bilayer. Experiments carried out with acetate-*loaded* vesicles (data not shown) did not reveal significant differences from the data presented. Based on this result, we tend to exclude the asymmetrical distribution of proton acceptors as the cause of the proton transfer decrease.

Finally, it must be noted that we have used SUV. These vesicles are highly packed and present an inner curvature radius which differs from the outer curvature radius. This feature promotes the asymmetrical distribution of lipid components at the membrane surfaces. Thus, lipids with a larger polar head, as NAPH-PE, would locate preferentially at the outer surface of the membrane.

The effect of the lipid gel-to-liquid-crystalline phase transition on proton transfer has been revealed by the steady-state fluorescence spectra recorded as a function of temperature (Figs. 5 and 6). The temperature-dependent structural properties of small unilamellar vesicles may well explain this result. Below the phase transition, the structure of the bilayer is compact, the surface area *per* lipid molecule small, and the solvation water is very low. Altogether these features result in caging the neutral fluorophores (i.e., nonionized naphthol) and limit the acetate accessibility. Above the phase transition, the structure of the bilayer is dynamic, the surface area *per* lipid molecule is larger, and the solvation water is higher. These changes result in uncaging the nonionized fluorophores and increase the acetate accessibility.

This interpretation is supported by the steady-state fluorescence anisotropy measurements shown in Fig. 8. Below the phase transition of both the DML and the DPL vesicles, the rotational movements of the nonionized NAPH-PE species are restricted ($\langle r\rangle \approx 0.25$), whereas above the phase transition of both the DML and the DPL vesicles, the nonionized NAPH-PE species experience a more dynamic environment ($\langle r\rangle \approx 0.12$). These changes trace the different phase transitions of the two lipid systems. Nonetheless, comparison with the results obtained using DPH, a probe of the inner hydrophobic core of the bilayer, shows that NAPH-PE fluorophores reside in a different region of the bilayer. In particular, the broader *vs.* the sharper changes of the fluorescence anisotropies measured with NAPH-PE and DPH, respectively, can be related to the higher dynamics heterogeneity experienced by a probe bound to the polar head region than a probe embedded in the acyl-chain region of the lipid bilayer. Recently, molecular dynamics studies[48] have shown how, on going from the highly ordered L_β phase to the partially ordered liquid crystal $L_\alpha$phase, both the segmental acyl chains and the whole

lipid molecule (axial rotation and wobble) reorientational movements are affected. In this respect, NAPH-PE reflects the physical state of the bilayer as a reporter of the whole lipid molecule dynamics.

Since both the steady-state fluorescence intensity and the anisotropy studies presented here were performed in pure DML or DPL vesicles, a potential and relevant property of the fluorescent lipid analogue (i.e., preferential partitioning in gel/fluid lipid phases) has not been investigated. Further experiments can be carried out in which the lipid "melt" transition profiles are monitored at a single experimental temperature (between the DML and the DPL T_c) with vesicles prepared at different DML/DPL composition ratios.

Nonetheless, it is of interest to note that the combination of steady-state fluorescence intensity and anisotropy measurements has revealed that changes of the fluidity of the bilayer may influence the chemical properties and reactivity of groups at the membrane surface. These findings can help the understanding of the signal transduction mechanisms involved in many relevant biological processes.

Global ("target") analysis procedures to fit fluorescence decay surfaces directly in terms of rate constants for excited-state reactions have been developed by Beechem *et al.*[18,40] Using global analysis, the appropriate differential equations of this type of system have been reformulated into an eigenvalue–eigenvector problem. Rigorous error estimation in terms of confidence intervals is a major advantage of this procedure. In addition, these studies have clearly shown that for a rigorous representation of kinetic schemes and for obtaining appropriate (unique) solutions for the rate constants of excited-state reaction systems, decay fluorescence data must be collected under different experimental conditions (i.e., multiple pH's and temperatures, proton acceptor concentrations, etc.). More recently, methods based on numerical solution of the Debye–Smoluchowski equation have been developed.[49,50] They allow us to search directly for real physical quantities (diffusion coefficient, Debye radius, dielectric constants, etc.), and in this respect, they may represent the ultimate choice to analyze excited-state reaction systems. On the other hand, practical evaluation of the error contained in the input data (i.e., fluorescence decay curves) may be problematic using these procedures.

Given the instrumentation available and the features of the proton transfer reaction of NAPH-PE in lipid membranes, the fluorescence decay curves obtained at high acetate concentrations at both the emission wavelengths of protonated and deprotonated NAPH-PE have been analyzed using a multiexponential model. Based on this approximation, the recovered parameters represent the combined rate constants X and Y. Global analysis performed in terms of fluorescence decay parameters reveals a strong quenching of τ_1 (0.4 ns) in the absence of significant changes of τ_2 (5.9 ns), with recovered preexponential coefficients that are consistent with an excited-state reaction. It is worth pointing out that on changing the experimental temperature (i.e., to below and above the DML T_c), no major changes of the fluorescence lifetimes were found.

Although at present it is difficult to provide a more detailed definition of the kinetic system of NAPH-PE in lipid vesicles, the kinetic relationship between these rate constants ($X > Y$) confirms a two-state excited-state proton transfer process, in which deactivation from ROH* proceeds much faster than that from RO*.

The fluorescence parameters recovered may be explained either in terms of a pure excited-state proton transfer reaction (reversible case)[16] or in terms of a collisional quenching of the protonated species due to the interaction of nonionized NAPH-PE molecules with the surrounding lipids. It is interesting that, according to the first process mentioned, reversible excited-state proton transfer has been found for 2-naphthol at a low pH ($\leq$3).[16] In this respect, our data suggest that, in the liquid-crystalline phase, the lipid environment changes the equilibrium process of deprotonation of NAPH-PE. On the other hand, according to the second process mentioned, a physical effect of the lipid environment must be considered. In this case, an interaction on the nanosecond time scale of nonionized NAPH-PE molecules with the surrounding lipids would result in collisional quenching, whereas the more polar ionized species, possibly oriented to the solvent at the lipid–water interface of the membrane, are not affected by quenching mechanisms.

The data presented show that fluorescent molecules bound at the polar head region of phospholipid can provide new insights on the chemical and physical behavior of the lipid bilayer; in particular, dynamic information on relevant biological processes at the membrane surface can be obtained by the combination of steady-state and time-resolved fluorescence techniques.

ACKNOWLEDGMENTS

The synthesis of NAPH-PE was originally developed in the laboratory of Dr. Ludwig Brand at The Johns Hopkins University and we are grateful to Dr. Brand and Dr. L Davenport for their advice and continuous encouragement. We also wish to thank Drs. J. R. Knutson,

J. B. A. Ross, J. M. Beechem, and G. Sartor for helpful discussions. This work was supported by the Italian National Research Council (CNR) Target Project BTBS n.92.01215.PF70 to L.M. L.F. and C.M. were recipients of fellowships from AMPS, Parma, Italy, and from CNR, respectively.

REFERENCES

1. R. A. Badley, W. G. Martin, and H. Schneider (1973) *Biochemistry* **12**, 268–275.
2. J. Brunner and F. M. Richards (1980) *J. Biol. Chem.* **255**, 3319–3329.
3. D. K. Struck and R. E. Pagano (1980) *J. Biol. Chem.* **255**, 5404–5410.
4. Y. Takagaki, R. Radhakrishnan, C. M. Gupta, and H. G. Khorana (1983) *J. Biol. Chem.* **258**, 9128–9135.
5. B. K. Burnett, R. J., Robson, Y. Takagaki, R. Radhakrishnan, and H. G. Khorana (1985) *Biochim. Biophys. Acta* **815**, 57–67.
6. Y. Tanaka and A. J. Schroit (1986) *Biochemistry* **25**, 2141–2148.
7. J. R. Silvius, R. Leventis, P. M. Brown, and M. Zuckermann (1987) *Biochemistry* **26**, 4279–4287.
8. R. Pal, Y. Barenholz, and R. R. Wagnar (1988) *Biochemistry* **27**, 30–36.
9. H. J. Galla and J. Luisetti (1980) *Biochim. Biophys. Acta* **596**, 108–117.
10. J. R. Wiener, R. Pal, Y. Barenholz, and R. R. Wagner (1985) *Biochemistry* **24**, 7651–7658.
11. L. Davenport, J. R. Knutson, and L. Brand (1986) *Biochemistry* **25**, 1186–1195.
12. D. Hoekstra (1982) *Biochemistry* **21**, 1055–1061.
13. A. Weller (1961) *Prog. React. Kinet.* **1**, 189–214.
14. J. F. Ireland and P. A. H. Wyatt (1976) *Adv. Phys. Org. Chem.* **12**, 131–221.
15. N. M. Trieff and B. R. Sundheim (1965) *J. Phys. Chem.* **69**, 2044–2059.
16. W. R. Laws and L. Brand (1979) *J. Phys. Chem.* **83**, 795–802.
17. J. R. Knutson, D. G. Walbridge, and L. Brand (1982) *Biochemistry* **21**, 4671–4679.
18. J. M. Beechem, M. Ameloot, and L. Brand (1985) *Chem. Phys. Lett.* **120**, 466–472.
19. M. R. Loken, J. W. Hayes, J. R. Gohlke, and L. Brand (1972) *Biochemistry* **11**, 4779–4786.
20. W. R. Laws, G. H. Posner, and L. Brand (1979) *Arch. Biochem. Biophys.* **193**, 88–100.
21. A. Orstan, M. F. Lulka, B. Eide, P. H. Petra, and J. B. A. Ross (1986) *Biochemistry* **25**, 2686–2692.
22. R. Yam, E. Nachliel, S. Kiryati, and M. Gutman (1991) *Biophys. J.* **59**, 4–11.
23. E. Shimoni, Y. Tsfadia, E. Nachliel, and M. Gutman (1993) *Biophys. J.* **64**, 472–479.
24. M. Gutman, A. B. Kotlyar, N. Borovok, and E. Nachliel (1993) *Biochemistry* **32**, 2942–2946.
25. A. B. Kotlyar, N. Borovok, S. Kiryati, E. Nachliel, and M. Gutman (1994) *Biochemistry* **33**, 873–879.
26. P. Neyroz, L. Franzoni, A. Spisni, L. Masotti, and L. Brand (1992) *Chem. Phys. Lipids* **61**, 255–263.
27. C. W. F. McClare (1971) *Anal. Biochem.* **39**, 527–532.
28. H. O. Hauser (1971) *Biochem. Biophys. Res. Commun.* **45**, 1049–1055.
29. J. Brunner, P. Skrabal, and H. Hauser (1976) *Biochim. Biophys. Acta* **455**, 322–331.
30. L. T. Mimms, G. Zampighi, Y. Nozaki, C. Tanford, and J. A. Reynolds (1981) *Biochemistry* **20**, 833–840.
31. C. A. Parker and W. T. Rees (1960) *Analyst (London)* **85**, 587–600.
32. R. F. Chen and R. L. Bowman (1965) *Science (Washington, D.C.)* **147**, 729–732.
33. M. G. Badea and L. Brand (1979) *Methods Enzymol.* **75**, 378–425.
34. J. Yguerabide (1972) *Methods Enzymol.* **26**, 498–578.
35. D. V. O'Connor and D. Philips (1984) *Time-Correlated Single Photon Counting*, Academic Press, New York.
36. P. Wah, J. C. Auchet, and B. Donzel (1974) *Rev. Sci. Instrum.* **45**, 28–32.
37. P. R. Bevington (1969) *Data Reduction and Error Analysis for the Physical Sciences*, McGraw–Hill, New York.
38. A. Grinvald and I. Z. Steinberg (1974) *Anal. Biochem.* **59**, 583–598.
39. J. R. Knutson, J. M. Beechem, and L. Brand (1983) *Chem. Phys. Lett.* **102**, 501–507.
40. J. M. Beechem, M. Ameloot, and L. Brand (1985) *Anal. Instrum.* **14**, 379–402.
41. Th. Föster (1949) *Z. Elecktrochem.* **54**, 42–46.
42. L. Brand and W. R. Laws (1983) in *Time-Resolved Fluorescence Spectroscopy in Biochemistry and Biology*, Plenum, R. B. Cundall and R. E. Dale (Eds.), New York, pp. 319–339.
43. M. P. Andrich and J. M. Vanderkooi (1976) *Biochemistry* **15**, 1257–1261.
44. A. Gafni and L. Brand (1978) *Chem. Phys. Lett.* **58**, 346–350.
45. J. M. Beechem, J. R. Knutson, J. B. A. Ross, B. W. Turner, and L. Brand (1983) *Biochemistry* **22**, 6054–6058.
46. B. K. Selinger and C. M. Harris (1983) in R. B. Cundall and R. E. Dale (Eds.), *Time-Resolved Fluorescence Spectroscopy in Biochemistry and Biology*, Plenum, New York, pp. 729–737.
47. Y. N. Antonenko, O. N. Kovbasniuk, and L. S. Yaguzhinsky (1993) *Biochim. Biophys. Acta* **1150**, 45–50.
48. R. D. Pastor, R. M. Venable, and M. Karplus, (1991) *Proc. Natl. Acad. Sci. USA* **88**, 892–896.
49. E. Pines, D. Huppert, and N. Agmon (1988) *J. Chem. Phys.* **88**, 5620–5630.
50. D. Huppert, E. Pines, and N. Agmon (1990) *J. Opt. Soc. Am. B* **7**, 1545–1550.